Atmospheric Pollution Research 14 (2023) 101845

Contents lists available at ScienceDirect

Atmospheric Pollution Research

journal homepage: www.elsevier.com/locate/apr

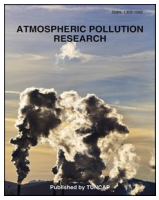

Exploring the acid neutralizing effect in rainwater collected at a tropical urban area: Central Valley, Costa Rica

Germain Esquivel-Hernández [a,*], Ricardo Sánchez-Murillo [b], Diego Villalobos-Córdoba [a], Lucilena Rebelo Monteiro [c], Mario Villalobos-Forbes [a], Rolando Sánchez-Gutiérrez [a], Marycel E.B. Cotrim [c], Ioannis Matiatos [d]

[a] Stable Isotopes Research Group and Water Resources Management Laboratory, Universidad Nacional Costa Rica, P.O. Box 86-3000, Heredia, Costa Rica
[b] Department of Earth and Environmental Sciences, University of Texas, Arlington, TX, 76019, USA
[c] Instituto de Pesquisas Energéticas e Nucleares, IPEN/CNEN Av. Prof. Lineu Prestes 2242 – Cidade Universitária, CEP 05508-000, São Paulo, SP, Brazil
[d] Hellenic Centre for Marine Research, 46.7 km of Athens-Sounio Ave, 19013, Anavissos, Attikis, Greece

ARTICLE INFO

Keywords:
Urban area
Rainwater
Chemical composition
Stable carbon isotopes
Dissolved inorganic carbon

ABSTRACT

We report on the chemical and the carbon isotopic composition of dissolved inorganic carbon (DIC) of rainwater collected between May and October 2020 in the Central Valley, Costa Rica. Precipitation samples were collected daily ($N = 55$) and analyzed for major ions, DIC, and $\delta^{13}C_{DIC}$. Significant correlation ($p < 0.05$) between main acidic (SO_4^{2-} and NO_3^-) and major alkaline (Ca^{2+} and NH_4^+) species confirmed a very effective acid neutralization effect in rainwater (average pH: 5.90 ± 0.74). Significant temporal variations ($p < 0.05$) of $\delta^{13}C_{DIC}$ indicated the contribution of carbonate salts in rainwater from May to October but also CO_2 dissolution at the beginning of the wet season (May), probably due to increased CO_2 emissions from soil degassing. Temporal changes of Ca^{2+} neutralization factors followed the observed changes in $\delta^{13}C_{DIC}$, which confirmed the high buffer capacity of precipitation in our study. HYSPLIT analysis also revealed long-range contributions of pedogenetic carbonates (e.g., Saharan dust) responsible for the acid neutralization capacity of rainwater (e.g., from July to September). Principal component analysis showed that four main factors explain 65% of the variance are: i) acid neutralization processes (Ca^{2+} neutralization factor), ii) marine salts (Cl^-, Na^+), iii) fossil fuels (SO_4^{2-}, NO_3^-), and iv) agriculture/fertilizers (NO_3^-, NH_4^+, K^+). Our study demonstrated that a combined approach of chemical, isotope, and statistical analysis techniques can help unravel the mechanism of acid neutralization of rainwater in tropical urban areas. This information has strong implications for future studies related with the impact of acid deposition on ecosystem functioning, water quality, and infrastructure degradation.

1. Introduction

Rainwater plays a key role in removing air pollutants and particulate matter from the atmosphere. Assessing the chemical composition of rainwater gives insights into air pollution, the relative contribution of different sources of atmospheric pollutants, and the potential impacts on terrestrial and marine ecosystems (Martins et al., 2019; Neal and Kirchner, 2000; Meng et al., 2019; Wang et al., 2012). However, the presence and concentration of the chemical constituents highly depend on the local meteorology, geography, and contribution sources (i.e., anthropogenic, terrestrial, and marine inputs) (Payus et al. 2020; Vier-a-Filho et al. 2013; Zeng et al., 2020). Acid rain has been a significant problem in North America and Europe due to historical high emissions of sulfur dioxide (SO_2) and nitrogen oxides (NO_x) from industrial activities and power generation, but regulatory measures and technological advancements have led to improvements of air quality and a reduction in acid rain occurrences in these regions (Vet et al., 2014). However, in developing economies there is an ongoing concern about the occurrence of acid rain if adequate pollution control measures are not implemented (Kumar et al., 2014; Mehr et al., 2019; Monteiro Porfírio et al., 2018). Thus, studies on precipitation chemistry should be systematically carried out at different spatial and temporal scales to help stakeholders determine scientific-based air quality mitigation strategies and management plans (Keresztesi et al., 2020).

Peer review under responsibility of Turkish National Committee for Air Pollution Research and Control.
* Corresponding author. Universidad Nacional Costa Rica Campus Omar Dengo, P.O. Box 86-3000, Heredia, Costa Rica.
E-mail address: germain.esquivel.hernandez@una.cr (G. Esquivel-Hernández).

https://doi.org/10.1016/j.apr.2023.101845
Received 12 April 2023; Received in revised form 12 July 2023; Accepted 13 July 2023
Available online 19 July 2023

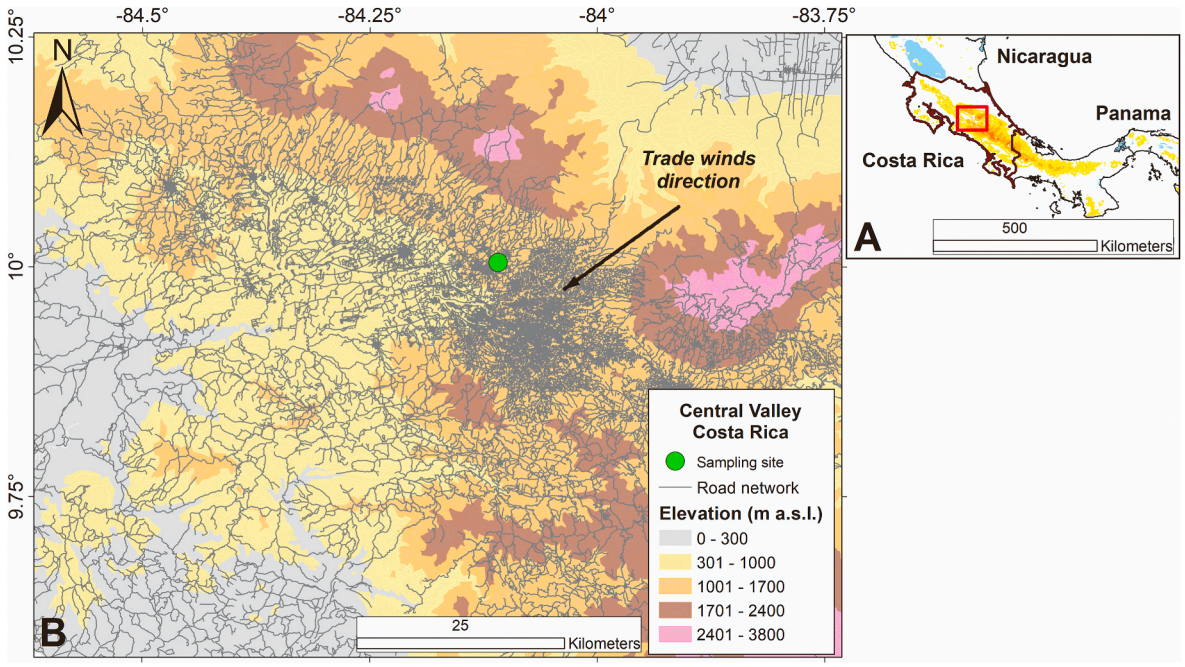

Fig. 1. A) The approximate location of the study region within the Costa Rican territory. B) The location of the precipitation sampling site in the Central Valley of Costa Rica. The available road system inside the valley and the dominant wind direction are shown as references.

In urban areas whereSO_2 and NO_x emissions are increased, acid precipitation has become a common concern of scientists, decision makers, and governmental institutions because it produces environmental disturbances in terrestrial and aquatic systems (i.e., mobilization of soil nutrients, increasing levels of toxicity due to higher concentration of species like aluminum in water bodies, and damage to foliar tissues of plants and trees), but also due to its indirect effects on human health (Keresztesi et al., 2020; Kumar et al., 2002; Li et al., 2022a; Vet et al.,

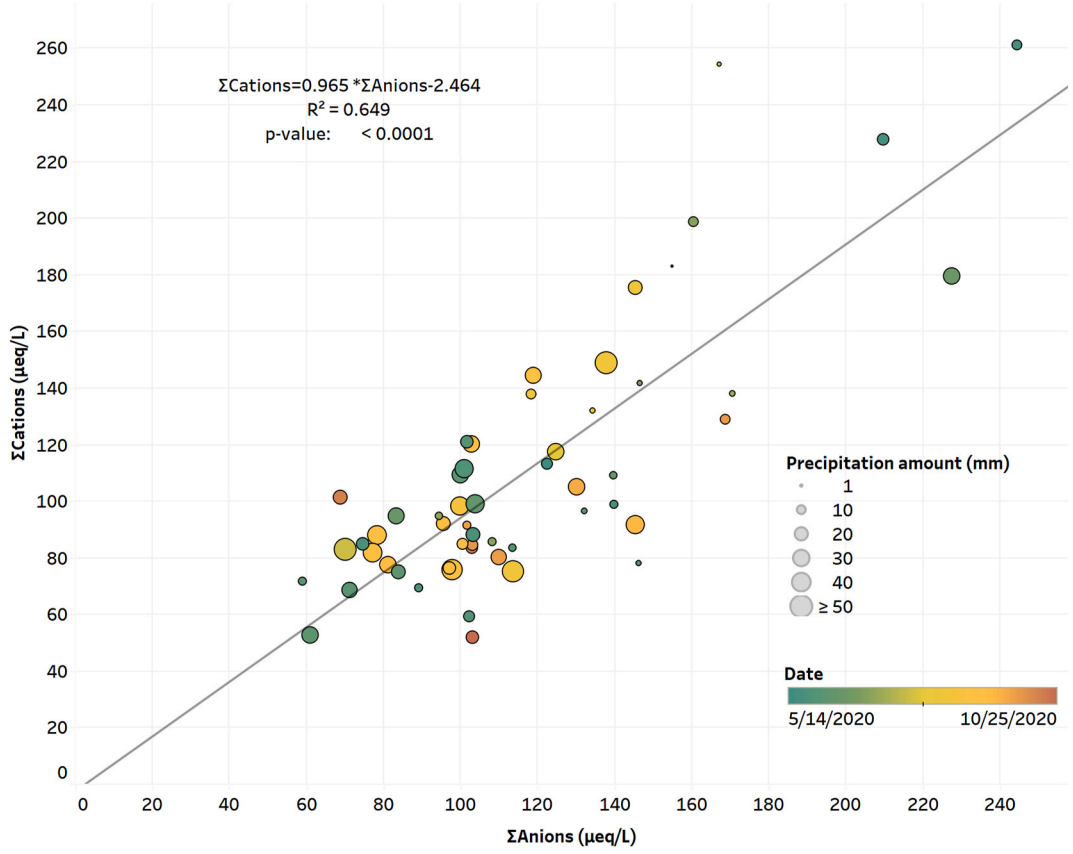

Fig. 2. Linear regression between the total anions and cations (µeq/L). Precipitation (as indicated by the dot size) and date (as indicated by the color code bar) are included as reference.

2014). Acidity and ion concentration in precipitation depend on the intensity of emissions sources, the removal efficiency of gases and aerosols, and the physical and chemical transformations that occur during rainout (in-cloud) and washout (below-cloud) (Herrera et al., 2009; Monteiro et al., 2021; Sharma et al., 2023; Shukla et al., 2008; Zeng et al., 2020, 2022). Overall, the acidity of precipitation is controlled by neutralization reactions with alkaline species from mineral dust (e.g., carbonates) and/or dissolved gases such as ammonia (NH_3). Hence, studies to clarify the acid-neutralization processes of precipitation are of interest because the abundance of alkaline particles (e.g., calcium, sodium, and magnesium) and NH_3 in the atmosphere can be timely and spatially variable. Up-to-date information is needed to assess the effectiveness of acid neutralization in precipitation as this process can diminish the potential negative impacts on the local environmental (Li et al., 2022b; Mehr et al., 2019; Wang et al., 2012).

The chemical composition of rainwater has been investigated around the world over the past years (Bisht et al., 2022; Keresztesi et al., 2020; Li et al., 2022a; Mehr et al., 2019; Qiu and Felix, 2021; Vet et al., 2014; Zeng et al., 2020). However, rainwater chemistry does not inform about the source contribution of atmospheric pollutants due to the intricated formation mechanisms and transformation processes. To overcome this limitation, the combined application of environmental isotopes with atmospheric chemistry has proven useful to better understand wet deposition and to characterize the sources and transformations of inorganic species inputs (Ciężka et al., 2016; Górka et al., 2011; Wu et al., 2021; Villalobos-Forbes et al., 2021; Passos et al., 2022). Dissolved inorganic carbon (Li et al., 2019) isotopes ($\delta^{13}C_{DIC}$) are widely used to study carbon sources and biogeochemical processes in aquatic systems (e.g., carbonate dissolution, soil/atmospheric CO_2 dissolution, carbon assimilation) (Pawellek and Veizer, 1994; Sánchez-Murillo et al., 2022; Wang et al., 2019). Regarding atmospheric applications, $\delta^{13}C_{DIC}$ values have been used to identify potential sources of DIC in urban precipitation (Górka et al., 2011).

The Central Valley of Costa Rica is characterized by the greatest urban conglomerate of the country and is formed by the four major cities of Costa Rica (~75% population, ~900 inhabitants per km^2). Anthropogenic emissions from local transportation and industrial emissions are mainly linked to fossil fuel combustion. Vehicles are responsible for 66% of fuel consumption (with ~75% of these vehicles using gasoline) and 54% of urban emissions. Unlike transportation, industrial activities are based on the consumption of other fuels like diesel which usually has high sulfur content (3500–4000 ppm; Herrera et al., 2009; Herrera-Murillo and Rodríguez-Román, 2009). However, past studies carried out in the Central Valley reported that the average pH measured in precipitation is not lower than the global average (pH 5.7, Balestrini et al., 2016; Bisht et al., 2022) for pollution-free areas (Herrera et al., 2009; Villalobos-Forbes et al., 2021). Our study aims to describe the processes, sources, and temporal variability involved in the acid neutralizing effect of precipitation in the main urban area of Costa Rica. This work uses a combined approach for characterizing the precipitation based on chemical, isotope, and statistical analysis from a wet season (2020) monitoring in the Central Valley of Costa Rica.

2. Methods

2.1. Study area

The sampling site was located at the main campus of Universidad Nacional, Costa Rica (Latitude: 10.005°, Longitude: 84.109°, 1100 m asl) within the main metropolitan area of Costa Rica, known as the Central Valley. As shown in Fig. 1B, the area surrounding the sampling site can be considered as representative of the urban conglomerate. The Central Valley is characterized by a dry season from December to April and a wet season from May to November. Two rainfall maxima are usually recorded during the wet season, one from May to June and one from September to October, which are interrupted by a rainfall decrease between July and August (known as the midsummer drought), due to intensification of the trade winds over the Caribbean Sea and travel from NE to SW inside the valley (Fig. 1B, Durán-Quesada et al., 2017; Maldonado et al., 2013). As the formation of polluted air over the urban conglomerate is enhanced during the wet season (May to November) by a reduction in the mixed layer height and a decrease in the intensity of the gas mixing dynamics in the atmospheric boundary layer Carballo-Chaves et al., 2020; Herrera et al., 2009; Villalobos-Forbes et al., 2021), precipitation sampling was only carried out during the wet season. (see Fig. 2).

3.2. Precipitation sampling

Precipitation samples (N = 55) were collected daily around 7:00–9:00 a.m. and between May and October 2020, using a bulk collector (Palmex Ltd., Croatia). The collector's funnel and the transfer line connected to the collector's vessel were rinsed with deionized water every day after the sample collection in order to minimize possible contamination from dry deposition. Samples were filtered using 0.45 μm polytetrafluorethylene (PTFE) syringe membranes and fractionated into two portions: i) 30 mL were stored at dark and frozen conditions (−10 °C) until isotopic analysis of dissolved inorganic carbon ($\delta^{13}C_{DIC}$) and ii) 30 mL were stored at dark and cool conditions (5 °C) until ion and alkalinity analysis at the Stable Isotopes Research Group facilities (Universidad Nacional, Costa Rica). The hydrogen ion activity (pH) and electrical conductivity were measured after sample collection using a Benchtop Multiparameter Meter Mi-180 (Milwaukee Instruments, USA). Hourly meteorological conditions were registered at the sampling site with a Vantage Pro2 weather station (Davis Instruments, Hayward, CA, USA). During the study period, precipitation samples were subjected to a quality control survey to evaluate possible degradation of ionic species (e.g., nitrate) during the collection and preservation of samples before analysis. An explanation of the quality control procedures is described in Esquivel-Hernández et al. (2023).

2.3. Chemical and isotopic analysis

The concentration of major cations and anions in precipitation samples was analyzed using a Dionex Ion Chromatograph ICS 5000+ (Dionex, CA). The following chemical parameters were quantified: nitrate (NO_3^-), chloride (Cl^-), sulphate (SO_4^{2-}), ammonium (NH_4^+), sodium (Na^+), calcium (Ca^{2+}), potassium (K^+), and magnesium (Mg^{2+}). To evaluate the quality of our data, the standard operating procedures described by the Global Atmospheric Watch Precipitation Chemistry Programme were applied (Allan, 2004). The ion difference (% ID) of each sample was calculated as follows:

$$\%ID = \frac{100 * (CE - AE)}{(CE + AE)} \quad (1)$$

where CE and AE are the sum of cations (in μeq/L) and the sum of anions (in μeq/L), respectively. Samples with ion differences greater than ±20% were flagged and checked for possible contamination issues (N = 6). These samples were related to pH values greater than 6.5 (i.e., carbonated samples) and/or low electrical conductivities (<10 μS/cm). The detection limits of anions were in the range 0.05–0.2 mg/L, whereas the detection limits of cations were between 0.03 and 0.1 mg/L.

Filtered aliquots (6 mL) were pipetted into Exetainer® vials. An automated DIC sample preparation system (Picarro AutoMate FX system, USA) was employed to inject a 10% phosphoric acid solution into each sealed vial to liberate CO_2 from the sample. Additionally, dry and ultra-pure nitrogen was bubbled through the acidified solution to flush the released CO_2 from the vial headspace. The CO_2 was captured into gas sampling bags of a Picarro LiaisonTM Universal Interface before being sent to a Cavity Ring Down Spectroscopy analyzer (CRDS, Picarro G2201-i). After each measurement, the instrument and the gas sampling

Table 1
Summary of chemical and isotopic parameters of precipitation samples (N = 55; VWM, volume-weighted mean; SD, standard deviation).

Variable	P	pH	EC	NO_3^-	Cl^-	SO_4^{2-}	DIC	δ^{13}C-DIC	NH_4^+	Ca^{2+}	Mg^{2+}	Na^+	K^+
	mm		μS/cm	μeq/L	μeq/L	μeq/L	μeq/L	‰	μeq/L	μeq/L	μeq/L	μeq/L	μeq/L
VWM		5.76	9.6	10.0	22.0	27.8	49.8	−11.3	16.7	42.2	16.8	12.5	11.1
Average	20.1	5.90	10.4	11.0	24.5	29.9	51.7	−11.8	18.9	44.6	16.8	12.9	13.3
Median	18.3	5.93	8.7	8.8	17.6	25.9	48.7	−10.5	17.4	35.0	15.6	10.4	9.4
SD	14.3	0.74	5.8	5.0	24.4	14.2	21.8	4.8	14.3	30.9	6.0	5.7	24.4
Maximum	64.3	7.29	37.4	28.2	161	65.8	122	−5.5	80.5	198	47.7	28.4	161
Minimum	1.0	4.58	2.5	7.5	4.4	13.9	0.0	−25.9	1.4	17.5	15.6	3.4	3.1

bag were purged with fully dry and ultra-pure nitrogen between successive $\delta^{13}C_{DIC}$ measurements. The corresponding uncertainty for $\delta^{13}C_{DIC}$ is ±0.1‰ (1σ). Calibration was done using the following standards: University of McGill, Canada: CO_2 mixing ratio: 1553 ppmv, $\delta^{13}CO_2 = -43.15‰$, Heredia's compressed air: CO_2 mixing ratio: 419.1 ppmv, $\delta^{13}CO_2 = -10.09‰$, NOAA gas standard: CO_2 mixing ratio: 394.85 ppmv, $\delta^{13}CO_2 = -8.292‰$.

Stable isotope compositions are expressed as $\delta^{13}C = (R_{sample}/R_{std} - 1)\cdot 1000$, where R is the $^{13}C/^{12}C$ ratio in a sample or standard (std) and reported in the delta-notation (‰) relative to VPDB scale (Craig, 1957). The total alkalinity of at least 10 mL of each sample (reported as HCO_3^-, μeq/L) was analyzed by titration using a standardized HCl solution (0.02 M), where the endpoint was estimated using a glass electrode at pH = 4.5.

2.4. HYSPLIT trajectory analysis

Based on the time and date of sample collection, backward trajectories were computed up to 96 h prior to the precipitation ended. Hybrid Single Particle Lagrangian Integrated Trajectory (HYSPLIT with GDAS 0.5° or GFS 0.25° input data) was used (Stein et al., 2015) in a two-step process (Fleming et al., 2012): First, fixed endpoint heights between 500 and 4000 m above ground were assessed and in a second step a linear model of their vertical levels against air temperature was used to interpolate and identify the 0 °C isotherm (i.e., the level where precipitation is expected to be formed, Monteiro et al., 2021). A total of 385 HYSPLIT trajectories were calculated for 55 rain events at seven different heights (500, 700, 900, 1000, 1500, 2500 and 4000 m above ground). Thus, by using different trajectory altitudes, we expect to decrease the trajectories uncertainties and improve the interpretation.

Table 2
Varimax rotation for principal component analysis (PCs, Factor 1 and 2, N = 55). PCs > |0.400| are in bold and are considered significant.

Variable	Factor 1	Factor 2	Factor 3	Factor 4
$Ca^{2+}/(NO_3^- + SO_4^{2-})$	**0.74**	−0.33	0.11	−0.09
Date	**0.68**	0.04	−0.01	0.12
Ca^{2+}/Na^+	**0.61**	**−0.50**	−0.38	−0.22
pH	**0.57**	**−0.56**	0.12	0.00
DIC	**0.57**	−0.48	0.20	0.34
δ^{13}C-DIC	**0.54**	0.06	−0.24	0.46
Ca^{2+}	0.34	**−0.66**	−0.35	−0.08
SO_4^{2-}/Na^+	−0.05	−0.23	**−0.72**	−0.18
Cl^-/Na^+	−0.15	**−0.60**	0.42	**−0.56**
$NH_4^+/(NO_3^- + SO_4^{2-})$	−0.33	−0.21	**0.48**	**0.65**
K^+	−0.34	**−0.50**	**0.55**	**−0.48**
H^+	−0.38	**0.52**	−0.21	−0.10
NO_3^-	−0.40	**−0.57**	−0.31	0.10
Cl^-	−0.42	**−0.55**	**0.48**	−0.44
NH_4^+/NO_3^-	**−0.49**	−0.18	0.28	**0.63**
NSSF SO_4^{2-}	**−0.53**	**−0.49**	**−0.63**	0.04
EC	**−0.53**	0.09	−0.07	−0.14
SO_4^{2-}	**−0.55**	**−0.49**	**−0.61**	0.05
Na^+	**−0.58**	−0.09	0.16	0.17
NH_4^+	**−0.59**	−0.48	0.00	**0.56**
% of total variability	23.09%	17.87%	12.62%	11.35%

2.5. Data analysis

2.5.1. Neutralization and enrichment factors

We calculated the Ca^{2+} and NH_4^+ neutralization factors following Zeng et al. (2020, 2022) and Keresztesi et al. (2020). These two factors indicate the relationship of the basic ions (Ca^{2+} or NH_4^+) to that of the main acidic ions (SO_4^{2-} and NO_3^-) as follows:

$$\frac{Ca^{2+}}{NO_3^- + SO_4^{2-}} = \frac{[Ca^{2+}]}{[NO_3^-] + [SO_4^{2-}]} \quad (2)$$

$$\frac{NH_4^+}{NO_3^- + SO_4^{2-}} = \frac{[NH_4^+]}{[NO_3^-] + [SO_4^{2-}]} \quad (3)$$

where the ion concentrations, namely $[Ca^{2+}]$, $[NH_4^+]$, $[SO_4^{2-}]$, and $[NO_3^-]$, are expressed in μeq/L. We also estimated the sea salt and non-sea salt fractions of sulphate (%$SS_{sulphate}$ and %$NSS_{sulphate}$, respectively). The marine contribution to the sulphate concentration in precipitation was calculated as follows:

$$\%SS_{sulphate} = \frac{100 * (Na^+)_{rain}\left(\frac{SO_4^{2-}}{Na^+}\right)_{seawater}}{(SO_4^{2-})_{rain}} \quad (4)$$

where $(Na^+)_{rain}$ is the concentration of sodium in the precipitation, $(SO_4^{2-}/Na^+)_{seawater}$ is the ratio of sulphate in seawater, and $(SO_4^{2-})_{rain}$ is the concentration of the respective ion. The non-sea salt fraction (%$NSS_{sulphate}$) is assumed to correspond to 100-%$SS_{sulphate}$. Given the proximity of the Caribbean Sea and the Pacific Ocean to the Central Valley (~75–100 km), sea salt is expected to contribute to the total Na^+ and Cl^- concentrations in the precipitation of the Central Valley. The average Na^+/Cl^- ratio in the collected precipitation (0.73) was indeed very similar to corresponding ratio in seawater of 0.86 (Keresztesi et al., 2020). Thus, we selected sodium as the reference element to approximate the contribution of sea salt species to the ion composition of precipitation (Allan, 2004).

2.5.2. Statistical analysis

We applied the Kruskal-Wallis one way analysis of variance (ANOVA) on Ranks followed by Dunn's method to assess differences in the carbon isotopic of DIC and chemical variables between the sampling periods (i.e., monthly data). Pearson's correlation analysis was calculated to identify potential relationships between ion concentrations, derived parameters (i.e., neutralization factors and %$NSS_{sulphate}$), and carbon isotopic composition of dissolved inorganic carbon in precipitation. Statistical analyses (α = 0.05) were done using SigmaPlot software 11.0. To identify the relationships between the chemical variables in rainwater (Table 2), a Principal Component Analysis (PCA) was applied (Abdi and Williams, 2010), with the aim to characterize the temporal variability (i.e., date of sampling, Table 2) of the variables and to discriminate potential ion sources and atmospheric processes. Prior to the application of the PCA, a Kaiser Meyer Oklin test (KMO) and a Bartlett's test of sphericity (BTS) were applied to assess the suitability of the matrix (Steiner and Greider, 2020). The overall result of the KMO test was >0.5 which confirms the data suitability for the PCA. The BTS

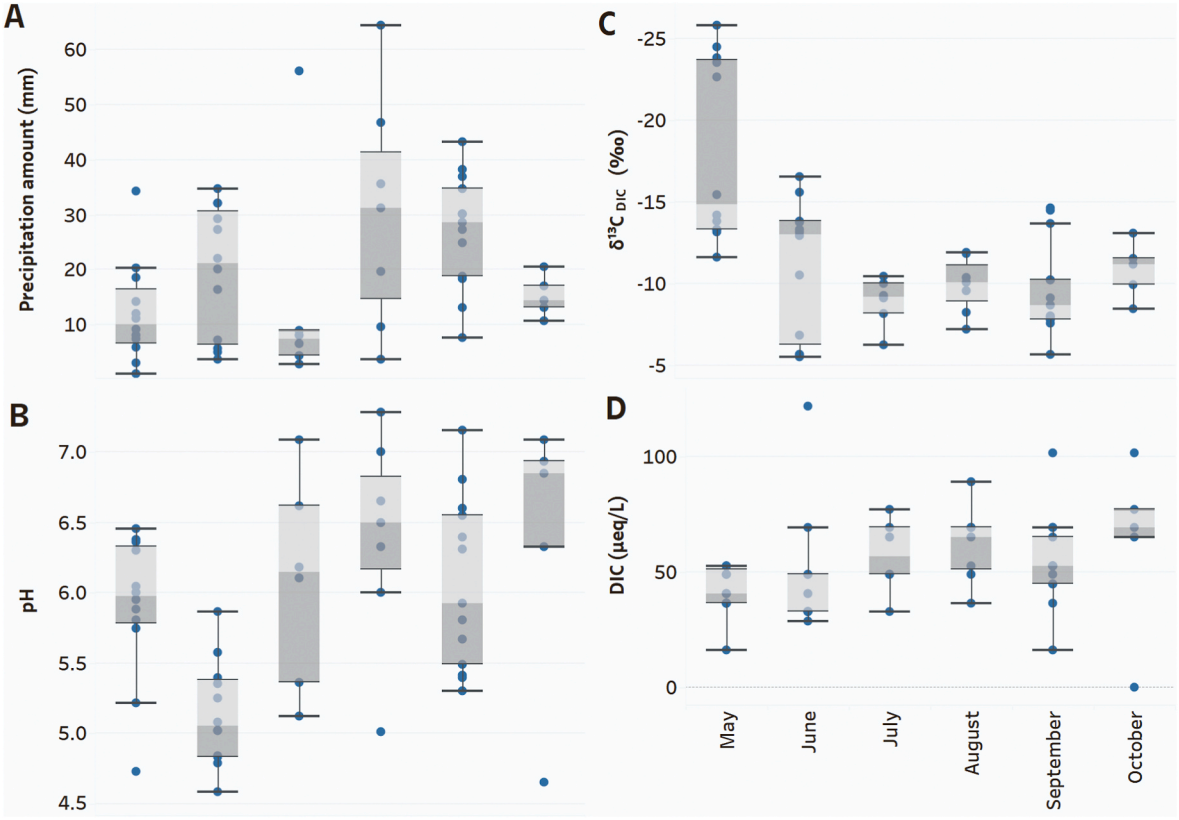

Fig. 3. Boxplots of monthly variations of A) rainfall (in mm), B) pH, C) $\delta^{13}C_{DIC}$ (in ‰), and D DIC (µeq/L).

test result was significant ($Chi^2 = 970$, $p < 0.001$, $df = 13$) which rejects the hypothesis the variable matrix is an identity matrix and confirms that the variables are significantly correlated.

3. Results

3.1. Chemical composition of precipitation and temporal variations

The quality control of the data showed that the implementation of practice guidelines for the sampling and chemical analysis of rainwater (Allan, 2004) is important to generate reliable results, as evidenced by

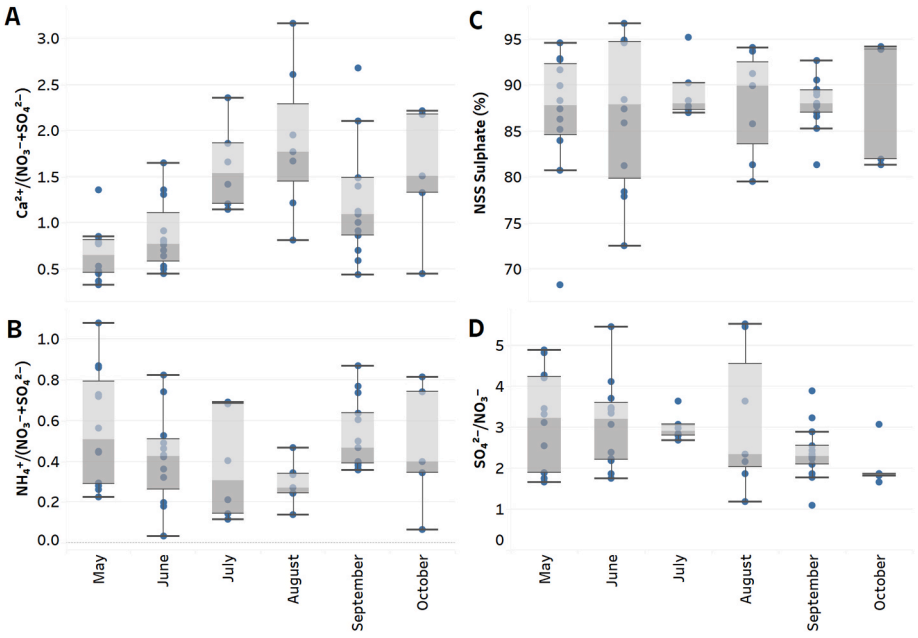

Fig. 4. Boxplots of monthly variations of A) the calcium neutralization factor ($Ca^{2+}/NO_3^- + SO_4^{2-}$), B) the ammonium neutralization factor ($NH_4^+/NO_3^- + SO_4^{2-}$), C) $NSS_{sulphate}$ (in %), and D) SO_4^{2-}/NO_3^- ratio.

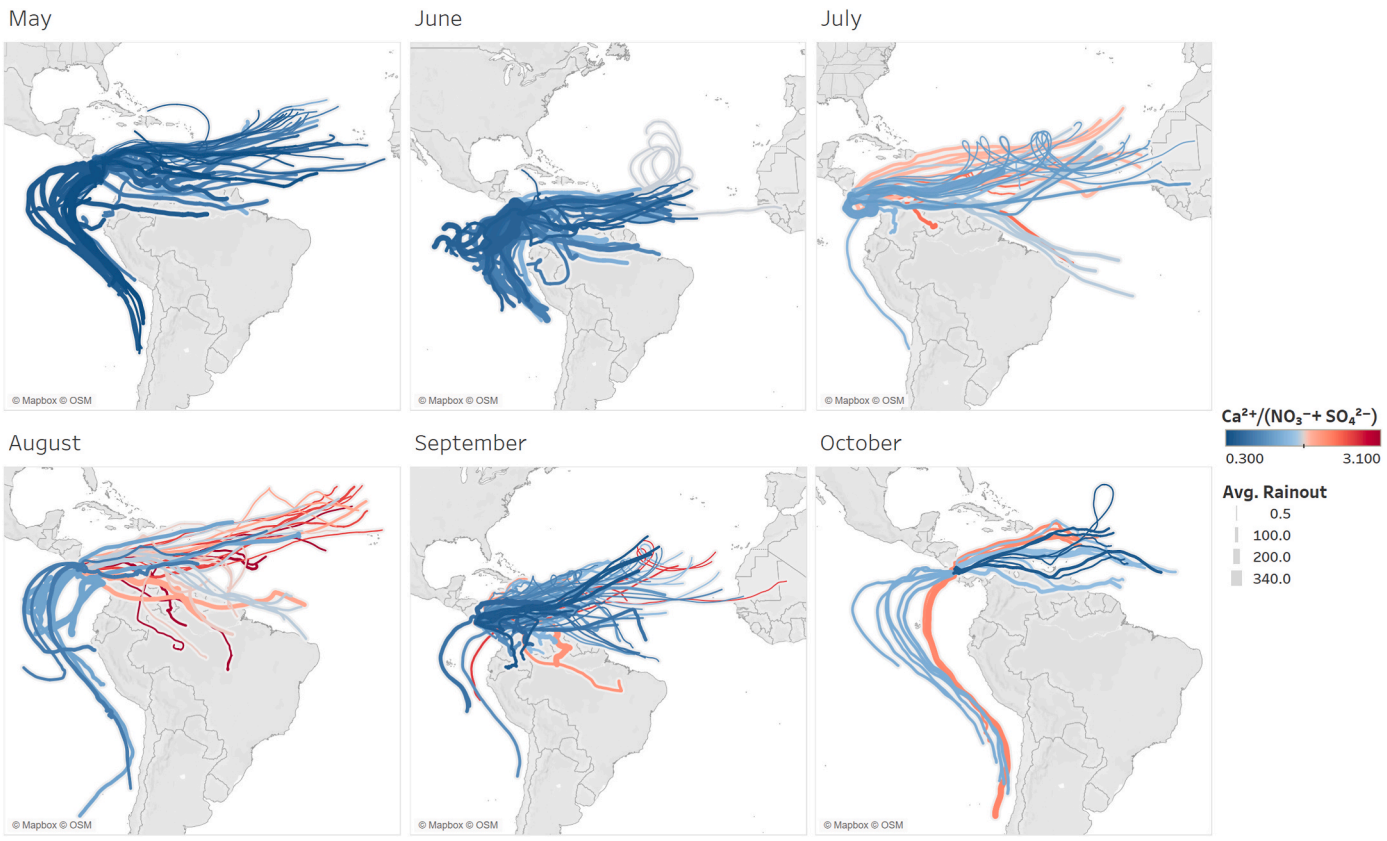

Fig. 5. Backward HYSPLIT trajectories calculated as per temporal variations of Ca^{2+} neutralization factor in precipitation of the Central Valley, Costa Rica. Trajectories are color coded by the corresponding Ca^{2+} neutralization factor value and by the average rainout (thickness of the trajectory line).

the ion balance calculations (Fig. 1). The % ID values of precipitation samples ranged from −32.9% to +20.7% (average: 3.9% ± 11.6%). Around 62% of the samples showed negative % ID values (i.e., cation deficit). As shown in Fig. 1, a significant linear regression between the sum of cations and anions, with a slope ~1 and an intercept close to zero, was identified. Overall, the rainwater samples were related to moderate-to-intense precipitation events with rainfall amounts up to 64.3 mm, which led to relatively low EC values (up to 7.29 μS/cm, Table 1).

The pH and chemical composition of rainwater indicated an effective neutralization effect. Rainwater pH exhibited a maximum value of 7.29 (average: 5.90 ± 0.74) with 38% of the samples being classified as acidic (pH < 5.60; Balestrini et al., 2016). The cations with the highest concentration were Ca^{2+} and NH_4^+, whereas the anions with the highest concentrations were SO_4^{2-} and Cl^-. As for SO_4^{2-} concentrations, the average $\%NSS_{sulphate}$ was 88% ± 6% with values up to 97%. The dissolved inorganic carbon concentrations in rainwater (average: 51.7 ± 21.8 μeq/L) were mostly related with $\delta^{13}C_{DIC}$ values between −5‰ and −15‰ (75%) and only 15% of the samples showed $\delta^{13}C_{DIC}$ values lower than −15‰ (up to −25.9‰). The average $\delta^{13}C_{DIC}$ value was −11.8 ± 4.8‰.

Monthly variations in key parameters (i.e., pH, DIC, $\delta^{13}C_{DIC}$, and neutralization factors) evidenced an effective acid neutralization effect in precipitation. Monthly pH values were significantly lower ($p < 0.001$) at the beginning of the wet season when the precipitation amount was high (i.e., washout effects, Fig. 3A and B). The lowest pH value was recorded in June, with a median value of 5.05, which was significantly lower ($p < 0.05$) than the highest pH value detected in October, with a median value of 6.85. No significant differences were found in the median pH values from July to October (Fig. 3B). A significant difference ($p < 0.001$) between monthly $\delta^{13}C_{DIC}$ values was identified. The lowest $\delta^{13}C_{DIC}$ values were recorded in May with a median value of −14.8‰. This value is significantly lower ($p < 0.05$) than the corresponding median values recorded in July, August, and September, which range from −10.1‰ to −8.7‰ (Fig. 3C). From June to October, the $\delta^{13}C_{DIC}$ values were relatively constant. A significant difference ($p < 0.05$) in the median DIC concentrations from May to October was identified (Fig. 3D). We observed an increment of DIC in rainwater throughout the wet season which is probably related to the input of neutralizing species (e.g., carbonates or NH_3) as reflected in the high median pH values recorded from July to November (Radha et al., 2022; Wang et al., 2019). The lowest median DIC concentrations were recorded in May (32.5 μeq/L) whereas the highest median concentration was detected in October (69.0 μeq/L, Fig. 3D).

An interesting trend was observed in the Ca^{2+} and NH_4^+ neutralization factors. Significant differences ($p < 0.001$) among monthly Ca^{2+} neutralization factors were identified but no significant variations ($p > 0.05$) in the corresponding NH_4^+ neutralization factors (Fig. 4A and B). As for Ca^{2+} neutralization factors, the median values calculated for May and June (0.65 and 0.77, respectively) were significantly lower ($p < 0.05$) than the median values recorded for the period from July to October (with values > 1). In this last period, no significant differences ($p > 0.05$) were identified in these neutralization factors, which were in the range 1.54–1.77. Unlike the Ca^{2+} neutralization factors, the NH_4^+ neutralization factors were mostly <0.5 (Fig. 4B), with the lowest median value observed in July (0.31) and the highest one in May (0.51). Thus, the acid neutralization process is controlled by both Ca^{2+} salts and NH_3 at the beginning of the wet season but it is predominantly dictated by Ca^{2+} species as neutralizing agents during the rest of the rainy period.

The SO_4^{2-}/NO_3^- ratio and the non-sea salt fraction of sulphate ($\%NSS_{sulphate}$) were calculated to explore the contribution of anthropogenic sources to atmospheric precipitation in the Central Valley (Herrera et al., 2009; Vet et al., 2014). Overall, no significant difference at $p > 0.05$ were observed in the median values of SO_4^{2-}/NO_3^- ratios and %

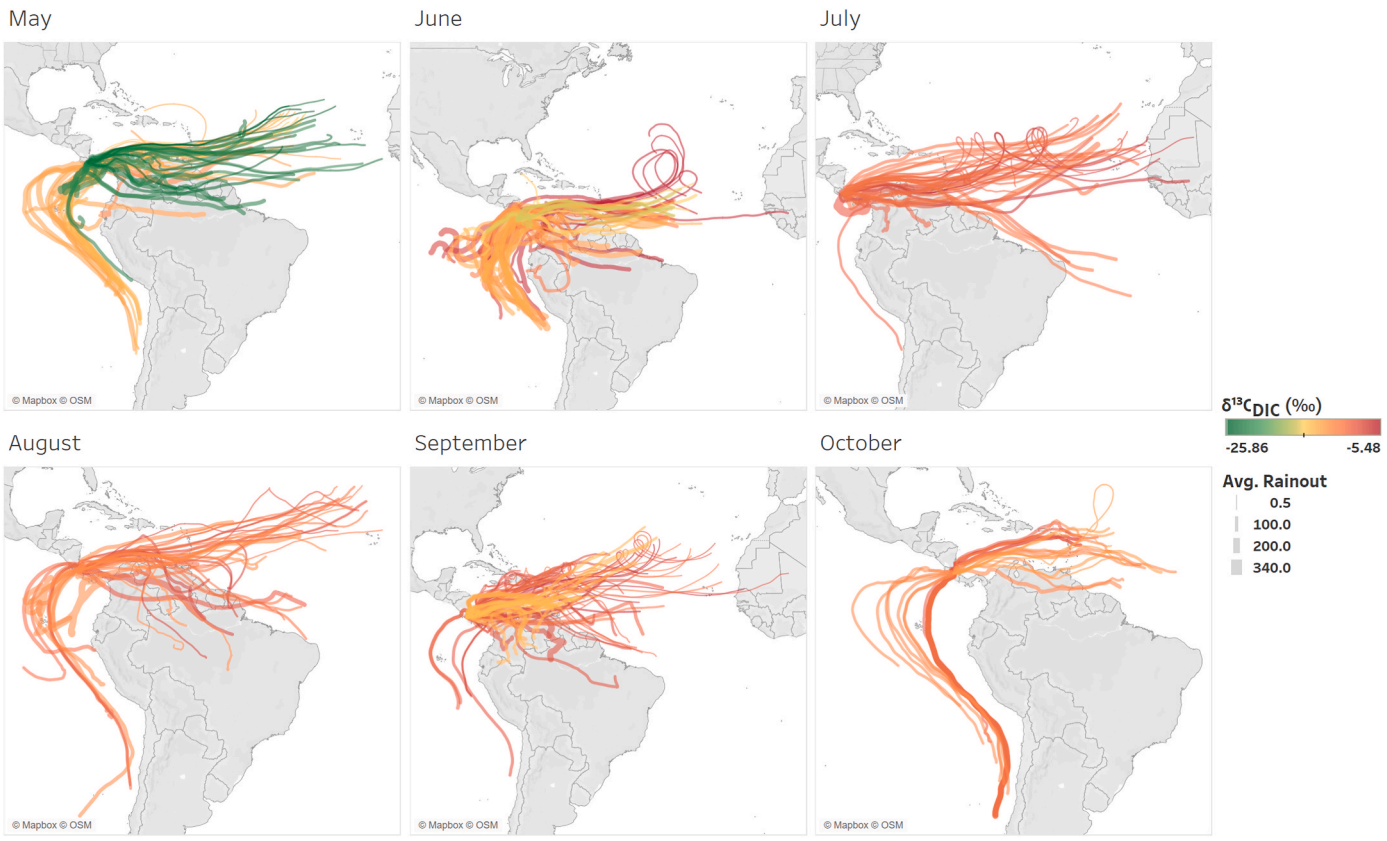

Fig. 6. Backward HYSPLIT trajectories calculated as per temporal variations of $\delta^{13}C_{DIC}$ (in ‰) in precipitation of the Central Valley, Costa Rica. Trajectories are color coded by the corresponding Ca^{2+} neutralization factor value and by the average rainout (thickness of the trajectory line).

$NSS_{sulphate}$ (Fig. 4C and D). The lowest median SO_4^{2-}/NO_3^- ratio was recorded in October (1.87), whereas the highest ratio was found in May (3.22). In turn, the lowest median $\%NSS_{sulphate}$ was registered in May (87.8) and the highest one was in October (93.8).

3.2. Air mass trajectories and acid neutralization

The HYSPLIT analysis for the Central Valley between May and October revealed that most of the air masses were related to short-range trajectories. These air masses mostly travelled over the central/southern Caribbean Sea basin and the central Pacific Ocean (Figs. 5 and 6). However, the incursion of long-range air masses that travelled over the central Atlantic Ocean and the southern Pacific Ocean before reaching the sampling site was identified. As reported above, there were significant differences among monthly values of Ca^{2+} neutralization factors and $\delta^{13}C_{DIC}$ values. Thus, the air mass trajectory patterns shown in Figs. 5 and 6 suggested that the significant increase in the median Ca^{2+} neutralization factors up to 1.51 and in the median $\delta^{13}C_{DIC}$ values up to −8.67‰, mostly from July to September, were related with long-range transport of acid neutralizing species to the Central Valley of Costa Rica, such as aerosols rich in crustal elements or pedogenetic carbonates from the Saharan desert (Oduber et al., 2020; Yu et al., 2021).

3.3. Correlation analysis

The correlation analysis between main acidic species (e.g., NO_3^- and SO_4^{2-}) with neutralizing species like Ca^{2+} and NH_4^+ and also with DIC concentrations provided evidence of the acid neutralizing effect in the precipitation of the Central Valley. We found a significant correlation between $NO_3^- + SO_4^{2-}$ and $Ca^{2+}+NH_4^+$ ($r = 0.599$, $p < 0.001$). On a monthly basis, the correlation between these ions was significant at the start of the wet season, namely in May ($r = 0.647$, $p < 0.05$), June ($r = 0.820$, $p < 0.01$) and in July ($r = 0.964$, $p < 0.01$). However, no correlation was found during the rainiest period (from August to October, Fig. 7A). A significant but weaker correlation between DIC and $Ca^{2+}+NH_4^+$ ($r = 0.316$ $p < 0.05$) was also detected. This correlation was only significant in June ($r = 0.819$, $p < 0.001$) and no correlations were found in May and from August to October (Fig. 7B). A significant but rather weak correlation between $\delta^{13}C_{DIC}$ and DIC (0.378, $p < 0.01$) was identified. However, no significant correlations were identified after disaggregating the data by month (Fig. 8A). A significant but weak correlation (0.356, $p < 0.05$) was found between $\delta^{13}C_{DIC}$ and the Ca^{2+} neutralization factor. When examined on a monthly basis, the correlation was higher in May ($r = 0.590$, $p < 0.05$) and September ($r = 0.938$, $p < 0.01$), but no correlation was found from June to August and in October (Fig. 8B).

3.4. Principal component analysis (PCA)

The PCA explained 65% of the observed variability (Table 2). This analysis was divided into four main factors. Factor 1 explained 23.09% of the system variability (Fig. 9A). This factor denoted a significant positive correlation between the sampling dates (0.68) and the Ca^{2+} neutralization factor (0.74), which indicated a neutralization increase towards the end of the wet season (Fig. 9B). DIC and $\delta^{13}C_{DIC}$ exhibited a weak (~0.5) association with this neutralization effect, which might indicate an increase of the terrestrial contribution at the end of the sampling period (e.g., October, Fig. 9B). In turn, at the beginning of sampling campaign (May), signals from secondary inorganic aerosols were indicated by the negative correlation (~-0.5) with ammonium and sulphate and the increase of EC. Overall, no precipitation amount effect was observed on these variables. Factor 2 explains 17.87% of the system variability. On this factor, the signals from marine (Cl^-, Na^+) and agricultural contributions like fertilizers (K^+, NO_3^-, NH_4^+) were mixed

Fig. 7. The monthly observed relationships between A) the sum of calcium and ammonium ($Ca^{2+} + NH_4^+$, µeq/L) and nitrate and sulphate ($NO_3^- + SO_4^{2-}$, µeq/L) and B) the dissolved inorganic carbon (DIC; µeq/L) and the sum of calcium and ammonium ($Ca^{2+} + NH_4^+$). The size of the dots corresponds to the precipitation amount in mm. Those panels marked with a red asterisk correspond to significant statistical correlations and the corresponding correlation coefficients and p values are also reported.

and inversely correlated with precipitation amount (Fig. 5A). These sources seemed not to be affected by seasonal variations. Together, Factors 3 and 4 explained 23.97% of the total variability and discriminated with a moderate correlation (~0.5) marine vs. fossil fuel (Factor 3) and agricultural (e.g., fertilizers, Factor 4) contributions.

4. Discussion

4.1. Processes controlling the acid neutralization in the precipitation of the main urban area of Costa Rica

Recent evidence suggested that acid deposition is a serious factor in the deterioration of water environments and ecosystems in urban areas, especially in Asia (Li et al., 2022b; Wu et al., 2021; Zeng et al., 2020; Zeng and Han, 2020, 2021). Unlike these urban areas, the almost constant temporal variation (i.e., monthly changes from May to October) of the ion composition in rainwater in the Central Valley of Costa Rica showed that the buffer capacity of rainwater was stable, that is, the input of acid compounds was effectively neutralized by the input of alkaline materials during the wet season (i.e., May to October). Our results are then comparable with other studies conducted in South America (i.e., Argentina and Brazil) and Iran, where a minority of precipitation samples had pH < 5.60 (Martins et al., 2019; Porfírio et al., 2018; Orué et al., 2019; Peikam and Jalali, 2021). Similar pH values < 5.60 were reported in urban areas in the USA (~87%, Keresztesi et al., 2020).

Our analysis confirmed that the origin of acidity of precipitation was mainly linked to the presence of inorganic acids (e.g., H_2SO_4, HNO_3) formed via photochemical oxidation as evidenced by the high % $NSS_{sulphate}$ values found in precipitation (up to ~97%). This finding agreed with another local study, where most (~96%) of the total precipitation acidity was due to SO_4^{2-} (Herrera et al., 2009). However, we also expected acidity contribution from organic acid species, which are very common in tropical rainwater (e.g., acetate, formate; Vet et al., 2014). The rainwater in the Central Valley was also loaded with alkaline species, such as carbonate salts and gaseous NH_3. However, given the relatively high pH of the rainwater, the dissolution of ammonia was probably reduced, which in turn was reflected in the reported cation deficit (i.e., NH_4^+ deficit). The significant correlation between $\delta^{13}C_{DIC}$ and the Ca^{2+} neutralization factor suggested that the dissolution carbonates (e.g., $CaCO_3$) was the main source of DIC in precipitation of the Central Valley of Costa Rica. The HYSPLIT analysis also indicated the possible incursion of long-range air masses, which transported carbonate salts to the Central Valley, contributing to the increase of the DIC concentration. Other authors have also analyzed the relationship between dissolved CO_2 and DIC in precipitation. For example, in Wroclaw (SW Poland), DIC was generated from other sources than the measured atmospheric CO_2 (Górka et al., 2011). In contrast, the total CO_2 concentration in rainwater collected in residential and urban areas of Kuwait was correlated with pH, alkalinity, and major ions (Radha et al., 2022). Thus, the low $\delta^{13}C_{DIC}$ values (up to −25.9‰) recorded at the beginning of the wet season (May 2020) suggested that soil organic matter oxidized to CO_2 (Pawellek and Veizer, 1994; Pataki et al., 2006; Horgby et al., 2019) contributed to the DIC in rainwater in the Central Valley and were probably related with the formation of rainfall from local recycled water vapor (i.e., evapotranspiration fluxes from surrounding tropical forests; Iraheta et al., 2021).

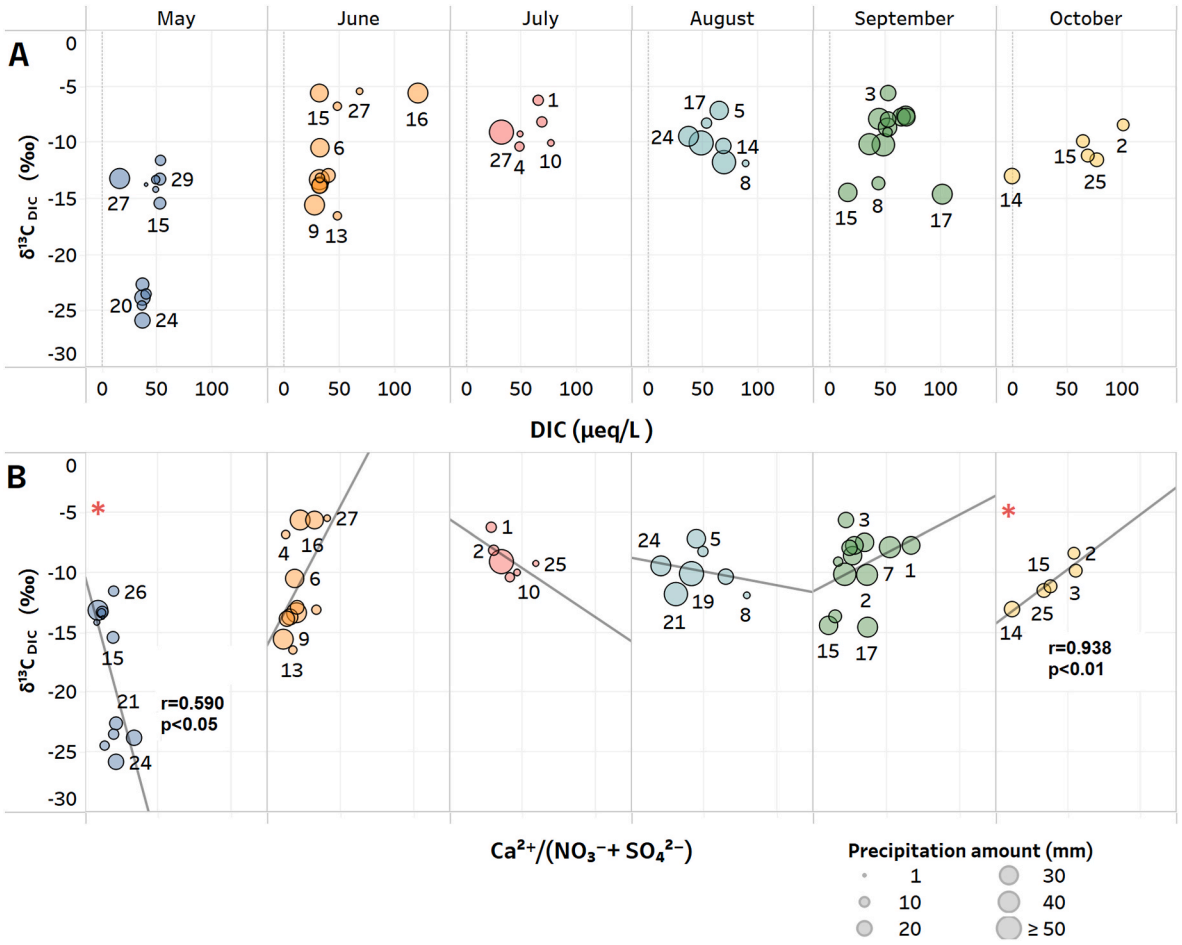

Fig. 8. The monthly relationships between the carbon isotope composition of dissolved inorganic carbon (δ^{13}C-DIC) and A) dissolved inorganic carbon (DIC; µeq/L) and B) the calcium neutralization factor ($Ca^{2+}/NO_3^- + SO_4^{2-}$). Those panels marked with a red asterisk correspond to significant statistical correlations and the corresponding correlation coefficients and p values are also reported.

4.2. Temporal variations of chemical species in rainwater and potential sources

PCA results and monthly variations of DIC, $\delta^{13}C_{DIC}$, and Ca^{2+} neutralization factor in precipitation clearly indicated distinct source contributions of ionic compounds in the precipitation of the Central Valley, such as salts from neutralization reactions (e.g., secondary inorganic aerosols), marine salts, fossil fuels, and agriculture. Overall, the significant difference between $\delta^{13}C_{DIC}$ values and Ca^{2+} neutralization factors between the beginning of the wet season (e.g., May and June) and the rest of study period indicated that the acid neutralization and DIC concentration in rainwater were controlled by inorganic carbon (mainly HCO_3^-) from carbonate dust with high Ca^{2+}content. Considering the air mass trajectory patterns observed during the study period, short-range air masses arriving at the Central Valley could be associated with the transport of anthropogenic sources, such as cement production emissions and local natural sources (e.g., alkaline particles from wind erosion). In turn, the incursion of long-range air masses was probably related with the deposition of pedogenetic carbonates (e.g., Saharan dust intrusions; Oduber et al., 2020). This interpretation was supported by the increasing trends in the $\delta^{13}C_{DIC}$ values and the Ca^{2+} neutralization factors. These variations indicated that the acid neutralization was mainly driven by the dissolution of carbonates with high $\delta^{13}C_{DIC}$ values (~−5‰, Pawellek and Veizer, 1994 and references herein) whereas the dissolution CO_2 with low high $\delta^{13}C_{DIC}$ values (~−25‰, Pawellek and Veizer, 1994 and references herein) may only be important at the beginning of the wet season when increasing soil emissions were emitted due to the onset of the rainy season. However, and as the rainy season established, the increase in precipitation amounts led to a decrease in the amount of HCO_3^- in rainwater due to a more effective scavenging of this ion via the formation carbonic acid (Keresztesi et al., 2020).

It is worth noting that long-range transport of dust carbonates deserves further investigation. To our knowledge, this is the first study reporting the wet deposition of dust from Africa in the Central Valley of Costa Rica. Overall, large quantities of African dust are routinely transported to southern US, the Caribbean Basin, and South America every year (McClintock et al., 2019; Prospero et al., 2020; Yu et al., 2021). The intrusion of these dusted air masses is linked to the deposition of phosphorus onto the deficient soils of the Amazonia but are also responsible for the input of crustal elements (e.g., Ca^{2+} and Mg^{2+}) and the increase of rainwater pH in Europe (higher than 6.5; Oduber et al., 2020). In fact, our sampling period coincided with a large African dust intrusion into the Caribbean Basin of June 2020 (Yu et al., 2021). Thus, we consider our study findings can be improved by extending the sampling period to include multiyear precipitation data and by collecting precipitation samples at different time resolutions (e.g., hourly sampling vs. 24-hour sampling). This information could then be used to better disentangle the contributions of local and distal carbonate salts sources (Monteiro et al., 2021).

The signals of anthropogenic sources (e.g., fossil fuels and agriculture) were difficult to separate from the natural contributions. For instance, marine contributions, represented by the Cl^-/Na^+ ratio in Fig. 9A, were better imprinted in the first months of the wet season (May and June) because of the predominant influence of the trade winds and

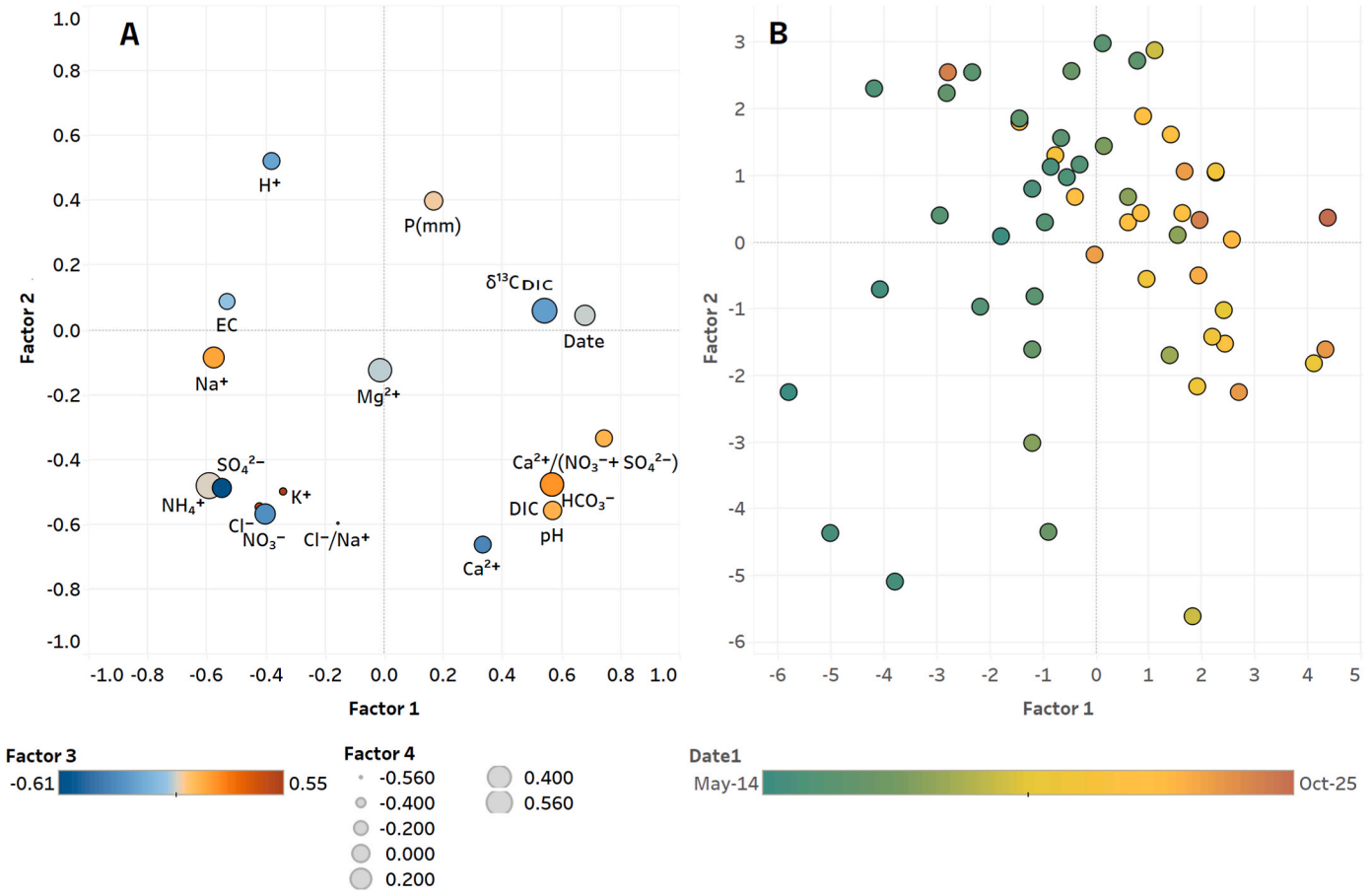

Fig. 9. Principal components for A) Factor 1 vs. Factor 2 loadings coded by Factor 3 values (color bar) and Factor 4 values (dot size) and B) Factor 1 vs. Factor 2 loadings as per date of sample collection. The date of sampling is coded by the color bar for the period May to October 2020.

to a lesser extent of cross-equatorial winds from the Caribbean Sea and the Pacific Ocean, respectively (Durán-Quesada et al., 2017). The chemical footprints of anthropogenic sources (e.g., SO_4^{2-}, NO_3^-, K^+) appeared to be inversely correlated with the precipitation amount. This agrees with the dilution effect in the ion concentrations reported for other regions (Payus et al. 2020; Qiu and Felix, 2021). Nevertheless, our sampling period coincided with intermittent lockdown conditions implemented in Costa Rica during 2020 due to the COVID-19 pandemic. Although no atmospheric chemistry data is available for Costa Rica during pandemic conditions, lockdown events have reduced the population-weighted concentration of nitrogen dioxide and particulate matter levels by about 60% and 31% in 34 countries (Venter et al., 2020) and may also decreased the formation of secondary pollutants like H_2SO_4 and HNO_3.

5. Conclusions

The ion chemistry and the $\delta^{13}C_{DIC}$ composition of rainwater collected at the Central Valley of Costa Rica was assessed to describe the acid neutralization processes and to investigate the temporal variability of the neutralizing effect. Rainwater composition confirmed that the origin of acidity of precipitation in the Central Valley of Costa Rica was mainly linked to the presence of inorganic acids (e.g., H_2SO_4, HNO_3), which were effectively neutralized by the input of alkaline species into the atmosphere (e.g., $CaCO_3$) and to a lesser extent by ammonia. HYSPLIT analysis indicated long-range dust inputs (e.g., pedogenetic carbonates from Saharan dust). The consistent high $\delta^{13}C_{DIC}$ values (~-5‰) also confirmed the contribution of carbonate salts. However, CO_2 dissolution also added to the DIC concentration and to the acid neutralization process, mainly at the beginning of the wet season, where low $\delta^{13}C_{DIC}$ values were recorded (~-25‰). Given the high buffer capacity found in the precipitation, the main source of ionic species was related to the formation of secondary inorganic species from acid neutralization, whereas the signals from marine, fossil fuels, and agricultural contributions were more difficult to distinguish. Interestingly, the calcium neutralization factor denoted a neutralization increase during the wet season, which was probably related to higher inputs of terrestrial sources.

Here, the combined use of chemical, isotope, and statistical analysis tools allowed studying the mechanism of acid neutralization in rainwater in a tropical urban area. Thus, we advise replicating our study in other tropical areas to expand the available information about this acid neutralizing effect. Sampling and analysis of rainwater during the intrusion of African dust is of great interest to better understand how the input of crustal elements, especially Ca^{2+}, help neutralize the rainwater in the Mesoamerican region. As for the Central Valley of Costa Rica, the continuing and systematic collection and analysis of rainwater is also recommended to compare these new data with the chemical composition of rainwater collected during COVID-19 pandemic lockdowns. Given the ongoing concern about the formation of acid rain in developing countries, our results also have interesting implications for future studies on precipitation chemistry in urban areas like the Central Valley of Costa Rica. Overall, studies on acid neutralization in precipitation can help assess the effectiveness of natural buffering systems in mitigating its ecological impacts and helping in water resources management and conservation efforts. Understanding acid neutralization processes is also of interest to manage infrastructure degradation. This information can aid in assessing the vulnerability of different materials to acid rain and

developing strategies for protection and restoration.

CRediT author contribution statement

Germain Esquivel-Hernández: Conceptualization; Formal analysis; Methodology; Project administration; Funding acquisition; Supervision; Writing - original draft. **Ricardo Sánchez-Murillo:** Data curation; Investigation; Project administration; Resources; Validation; Writing - review & editing. **Diego Villalobos-Cordoba:** Data curation; Formal analysis; Investigation; **Lucilena Rebelo Monteiro**: Visualization; Validation; Writing - review & editing. **Rolando Sánchez-Gutiérrez**: Data curation; Supervision. **Mario Villalobos-Forbes:** Data curation. **Marycel E.B. Cotrim**: Validation. **Ioannis Matiatos**: Writing - review & editing.

Declaration of competing interest

The authors declare the following financial interests/personal relationships which may be considered as potential competing interests: Germain Esquivel-Hernandez reports financial support was provided by International Atomic Energy Agency. Germain Esquivel-Hernandez reports a relationship with International Atomic Energy Agency that includes: funding grants. No additional or activities to declare.

Acknowledgments

GEH and RSM thank the Research Office of Universidad Nacional Costa Rica through Grant SIA-0339-18. This research was funded by the IAEA's Coordinated Research Project F32008 entitled "Global Monitoring of Nitrogen Isotopes in Atmospheric Waters", IAEA. We also thank Mr. Stefan Terzer- Wassmuth from IAEA for HYSPLIT trajectories automatic calculation and technical assistance on the subject.

Appendix A. Supplementary data

Supplementary data to this article can be found online at https://doi.org/10.1016/j.apr.2023.101845.

References

Abdi, H., Williams, L.J., 2010. Principal component analysis. WIREs Comp Stat 2, 433–459. https://doi.org/10.1002/wics.101.

Allan, M.A., 2004. Manual for the GAW Precipitation Chemistry Programme: Guidelines, Data Quality Objectives and Standard Operating Procedures. World Meteorological Organization, Geneva (Switzerland.

Balestrini, R., Delconte, C.A., Sacchi, E., et al., 2016. Wet deposition at the base of Mt Everest: seasonal evolution of the chemistry and isotopic composition. Atmos. Environ. 146, 100–112. https://doi.org/10.1016/j.atmosenv.2016.08.056.

Bisht, D.S., Srivastava, A.K., Singh, V., et al., 2022. High-Altitude air pollutants monitored from rainwater chemistry in the central himalaya. Water Air Soil Pollut. 233, 392. https://doi.org/10.1007/s11270-022-05855-8.

Carballo-Chaves, K., Villalobos-Forbes, M., Esquivel-Hernández, G., Sánchez-Murillo, R., 2020. Isotope composition of carbon dioxide and methane in a tropical urban atmosphere. Isotopes Environ Health Stud 56, 624–643. https://doi.org/10.1080/10256016.2020. 1803855.

Ciężka, M., Modelska, M., Górka, M., et al., 2016. Chemical and isotopic interpretation of major ion compositions from precipitation: a one-year temporal monitoring study in Wrocław, SW Poland. J Atmos Chem 73, 61–80. https://doi.org/10.1007/s10874-015-9316-2.

Craig, H., 1957. Isotopic standards for carbon and oxygen and correction factors for mass-spectrometric analysis of carbon dioxide. Geochim Cosmochim Acta 12, 133–149. https://doi.org/10.1016/0016-7037(57)90024-8.

Durán-Quesada, A.M., Gimeno, L., Amador, J.A., 2017. Role of moisture transport for Central American precipitation. Earth Syst. Dynamis 8, 147–161. https://doi.org/10.5194/esd-8-147-2017.

Esquivel-Hernández, G., Matiatos, I., Sánchez-Murillo, R., et al., 2023. Nitrate isotopes (δ15N, δ18O) in precipitation: best practices from an international coordinated research project. Isot Environ Healt S 59, 127–141. https://doi.org/10.1080/10256016.2023.2177649.

Fleming, Z.L., Monks, P.S., Manning, A.J., 2012. Review: untangling the influence of air-mass history in interpreting observed atmospheric composition. Atmos. Res. 104–105, 1–39. https://doi.org/10.1016/j.atmosres.2011.09.009.

Górka, M., Sauer, P.E., Lewicka-Szczebak, D., Jędrysek, M.O, 2011. Carbon isotope signature of dissolved inorganic carbon (DIC) in precipitation and atmospheric CO2. Environ. Pollut. 159, 294–301. https://doi.org/10.1016/j.envpol.2010.08.027.

Herrera, J., Rodríguez, S., Baéz, A.P., 2009. Chemical composition of bulk precipitation in the metropolitan area of Costa Rica, Central America. Atmos Res 94, 151–160. https://doi.org/10.1016/j. atmosres.2009.05.004.

Herrera-Murillo, J., Rodríguez-Román, S., 2009. Determination of anion concentration in total precipitation samples collected in San José, Costa Rica. Rev Int Contam Ambient 25, 65–72.

Horgby, Å., Segatto, P.L., Bertuzzo, E., et al., 2019. Unexpected large evasion fluxes of carbon dioxide from turbulent streams draining the world's mountains. Nat. Commun. 10, 4888. https://doi.org/10.1038/s41467-019-12905-z.

Iraheta, A., Birkel, C., Benegas, L., Ríos, N., Sánchez-Murillo, R., Beyer, M., 2021. A preliminary isotope-based evapotranspiration partitioning approach for tropical Costa Rica. Ecohydrol 14, e2297. https://doi.org/10.1002/eco.2297.

Keresztesi, A., Nita, I.A., Boga, R., et al., 2020. Spatial and long-term analysis of rainwater chemistry over the conterminous United States. Environ. Res. 188, 109872 https://doi.org/10.1016/j.envres.2020.109872.

Kumar, R., Rani, A., Singh, S.P., et al., 2002. A long term study on chemical composition of rainwater at dayalbagh, a suburban site of semiarid region. J. Atmos. Chem. 41, 265–279. https://doi.org/10.1023/A:1014955715633.

Kumar, P., Yadav, S., Kumar, A., 2014. Sources and processes governing rainwater chemistry in New Delhi, India. Nat. Hazards 74, 2147–2162. https://doi.org/10.1007/s11069-014-1295-0.

Li, X., Han, G., Liu, M., et al., 2019. Hydrochemistry and Dissolved Inorganic Carbon (DIC) Cycling in a Tropical Agricultural River, Mun River Basin, Northeast Thailand. Int J Environ Res Public Health 16, 3410. https://doi.org/10.3390/ijerph16183410.

Li, J., Wu, H., Jiang, P., Fu, C., 2022a. Rainwater chemistry in a subtropical high-altitude mountain site, South China: seasonality, source apportionment and potential factors. Atmos. Environ. 268, 118786 https://doi.org/10.1016/j.atmosenv.2021.118786.

Li, R.F., Dong, X.Y., Xie, C., et al., 2022b. Long-term observations of the chemical composition, fluxes and sources of atmospheric wet deposition at an urban site in Xi'an, Northwest China. Environ. Monit. Assess. 194, 68. https://doi.org/10.1007/s10661-021-09737-0.

Maldonado, T., Alfaro, E., Fallas-López, B., Alvarado, L., 2013. Seasonal prediction of extreme precipitation events and frequency of rainy days over Costa Rica, Central America, using canonical correlation analysis. Advances in Geosciences 33, 41–52. https://doi.org/10.5194/adgeo- 33-41-2013.

Martins, E.H., Nogarotto, D.C., Mortatti, J., Pozza, S.A., 2019. Chemical composition of rainwater in an urban area of the southeast of Brazil. Atmos. Pollut. Res. 10, 520–530. https://doi.org/10.1016/j.apr.2018.10.003.

McClintock, M.A., McDowell, W.H., González, G., Schulz, M., Pett-Ridge, J.C., 2019. African dust deposition in Puerto Rico: analysis of a 20-year rainfall chemistry record and comparison with models. Atmos. Environ. 216, 116907 https://doi.org/10.1016/j.atmosenv.2019.116907.

Mehr, M.R., Keshavarzi, B., Sorooshian, A., 2019. Influence of natural and urban emissions on rainwater chemistry at a southwestern Iran coastal site. Sci. Total Environ. 668, 1213–1221. https://doi.org/10.1016/j.scitotenv.2019.03.082.

Meng, Y., Zhao, Y., Li, R., et al., 2019. Characterization of inorganic ions in rainwater in the megacity of Shanghai: spatiotemporal variations and source apportionment. Atmos. Res. 222, 12–24. https://doi.org/10.1016/j.atmosres.2019.01.023.

Monteiro, L.R., Terzer-Wassmuth, S., Matiatos, I., Douence, C., Wassenaar, L.I., 2021. Distinguishing in-cloud and below-cloud short and distal N-sources from high-temporal resolution seasonal nitrate and ammonium deposition in Vienna, Austria. Atmos. Environ. 266, 118740 https://doi.org/10.1016/j.atmosenv.2021.118740.

Neal, C., Kirchner, J.W., 2000. Sodium and chloride levels in rainfall, mist, streamwater and groundwater at the Plynlimon catchments, mid-Wales: inferences on hydrological and chemical controls. Hydrol. Earth Syst. Sci. 4, 295–310. https://doi.org/10.5194/hess-4-295-2000.

Oduber, F., Calvo, A.I., Castro, A., et al., 2020. Chemical composition of rainwater under two events of aerosol transport: a Saharan dust outbreak and wildfires. Sci. Total Environ. 734, 139202 https://doi.org/10.1016/j.scitotenv.2020.139202.

Orué, M.R., Gaiero, D., Kirschbaum, A., 2019. Seasonal characteristics of the chemical composition of rainwaters from Salta city, NW Argentina. Environ. Earth Sci. 78, 16. https://doi.org/10.1007/s12665-018-8007-0.

Passos, R.G., Matiatos, I., Monteiro, L.R., et al., 2022. Imprints of anthropogenic air pollution sources on nitrate isotopes in precipitation in a tropical metropolitan area. Atmos. Environ. 288, 119300 https://doi.org/10.1016/j.atmosenv.2022.119300.

Pataki, D., Bowling, D., Ehleringer, J., et al., 2006. High resolution monitoring of urban carbon dioxide sources. Geophys. Res. Lett. 33, L03813 https://doi.org/10.1029/2005GL024822.

Pawellek, F., Veizer, J., 1994. Carbon cycle in the upper Danube and its tributaries: $\delta^{13}C_{DIC}$ constraints. Isr. J. Earth Sci. 43, 187–194.

Payus, C.M., Jikilim, C., Sentian, J., 2020. Rainwater chemistry of acid precipitation occurrences due to long-range transboundary haze pollution and prolonged drought events during southwest monsoon season: climate change driven. Heliyon 6, e04997. https://doi.org/10.1016/j.heliyon.2020.e04997.

Peikam, E.N., Jalali, M., 2021. Chemical composition of rainwater at an urban and two rural stations in the west of Iran, Hamedan. Environ. Earth Sci. 80, 605. https://doi.org/10.1007/s12665-021-09865-3.

Porfírio, D., Monteiro, L.R., Lima da Costa, M., 2018. Rainwater geochemistry inside the Barcarena power station at the mouth of the Tocantins River. Environ Tech 41, 981–996. https://doi.org/10.1080/09593330.2018.1516801.

Prospero, J.M., Barkley, A.E., Gaston, C.J., et al., 2020. Characterizing and quantifying African dust transport and deposition to South America: implications for the

phosphorus budget in the Amazon Basin. Global Biogeochem. Cycles 34, e2020GB006536. https://doi.org/10.1029/2020GB006536.
Qiu, Y., Felix, J.D., 2021. Hurricane/tropical storm rainwater chemistry in the US (from 2008 to 2019). Sci. Total Environ. 798, 149009 https://doi.org/10.1016/j.scitotenv.2021.149009.
Radha, S.V.V.D., Sabarathinam, C., Al-Ayyadhi, N., et al., 2022. Spatial and temporal variation of dissolved CO_2 in rainwater from an arid region with special focus on its association with DIC and pCO_2. Environ. Earth Sci. 81, 113. https://doi.org/10.1007/s12665-022-10176-4.
Sánchez-Murillo, R., Gastezzi-Arias, P., Sánchez-Gutiérrez, R., Esquivel-Hernández, G., Pérez-Salazar, R., Poca, M., 2022. Exploring dissolved organic carbon variations in a high elevation tropical peatland ecosystem: cerro de la Muerte, Costa Rica. Front Water 3. https://doi.org/10.3389/frwa.2021.742780.
Sharma, A., Khare, P., Singh, N., Tiwari, S., Chate, D.M., Kumar, R., 2023. Anthropogenic aerosols in precipitation over the Indo-Gangetic basin. Environ. Geochem. Health 45, 961–980. https://doi.org/10.1007/s10653-022-01236-6.
Shukla, J.B., Misra, A.K., Sundar, S., Naresh, R., 2008. Effect of rain on removal of a gaseous pollutant and two different particulate matters from the atmosphere of a cityMath. Comput. Model. 48, 832–844. https://doi.org/10.1016/j.mcm.2007.10.016.
Stein, A.F., Draxler, R.R., Rolph, G.D., Stunder, B.J.B., Cohen, M.D., Ngan, F., 2015. NOAA's HYSPLIT atmospheric transport and dispersion modeling system. Bull Amer Meteor Soc 96, 2059–2077. https://doi.org/10.1175/BAMS-D-14-00110.1.
Steiner, M.D., Grieder, S.G., 2020. EFAtools: an R package with fast and flexible implementations of exploratory factor analysis tools. J. Open Source Softw. 5, 2521. https://doi.org/10.21105/joss.02521.
Venter, Z.S., Aunan, K., Chowdhury, S., Lelieveld, J., 2020. COVID-19 lockdowns cause global air pollution declines. Proc. Natl. Acad. Sci. USA 117, 18984–18990. https://doi.org/10.1073/pnas.200685311.
Vet, R., Artz, R.S., Carou, S., et al., 2014. A global assessment of precipitation chemistry and deposition of sulfur, nitrogen, sea salt, base cations, organic acids, acidity and pH, and phosphorus. Atmos. Environ. 93, 3–100. https://doi.org/10.1016/j.atmosenv.2013.10.060.
Vieira-Filho, M., Pedrotti, J.J., Fornaro, A., 2013. Assessment of potassium and sodium excesses in rainwater. In: Proceedings of the Community Modeling and Analysis Systems (CMAS) Conference (Espirito Santo, Brazil).
Villalobos-Forbes, M., Esquivel-Hernández, G., Sánchez-Murillo, R., Sánchez-Gutiérrez, R., Matiatos, I., 2021. Stable isotopic characterization of nitrate wet deposition in the tropical urban atmosphere of Costa Rica. Environ. Sci. Pollut. Res. 28, 67577–67592. https://doi.org/10.1007/s11356-021-15327-x.
Wang, Y., Yu, W., Pan, Y., Wu, D., 2012. Acid neutralization of precipitation in Northern China. J. Air Waste Manag. Assoc. 62, 204–211. https://doi.org/10.1080/10473289.2011.640761.
Wang, W., Li, S.L., Zhonga, J., et al., 2019. Understanding transport and transformation of dissolved inorganic carbon (DIC) in the reservoir system using $\delta^{13}C_{DIC}$ and water chemistry. J Hydrol 574, 193. https://doi.org/10.1016/j.jhydrol.2019.04.036.
Wu, Y., Liu, W., Xu, Y., et al., 2021. Multiple isotopic tracing for sulfate and base cation sources of precipitation in Hangzhou city, Southeast China: insights for rainwater acidification mechanism. Environ Pollut 288, 17770. https://doi.org/10.1016/j.envpol.2021.117770.
Yu, H., Tan, Q., Zhou, L., et al., 2021. Observation and modeling of the historic "Godzilla" african dust intrusion into the Caribbean Basin and the southern US in June 2020. Atmos. Chem. Phys. 21, 12359–12383. https://doi.org/10.5194/acp-21-12359-2021.
Zeng, J., Han, G., 2020. Rainwater chemistry reveals air pollution in a karst forest: temporal variations, source apportionment, and implications for the forest. Atmos 11, 1315. https://doi.org/10.3390/atmos11121315.
Zeng, J., Han, G., 2021. Rainwater chemistry observation in a karst city: variations, influence factors, sources and potential environmental effects. PeerJ 9, e11167. https://doi.org/10.7717/peerj.11167.
Zeng, J., Yue, F.J., Li, S.L., et al., 2020. Determining rainwater chemistry to reveal alkaline rain trend in Southwest China: evidence from a frequent-rainy karst area with extensive agricultural production. Environ Pollut 266, 115166. https://doi.org/10.1016/j.envpol.2020.115166.
Zeng, J., Han, G., Zhang, S., et al., 2022. Rainwater chemical evolution driven by extreme rainfall in megacity: implication for the urban air pollution source identification. J. Clean. Prod. 372, 133732 https://doi.org/10.1016/j.jclepro.2022.133732.